



**HAL**  
open science

# INFLUENCE OF AUXETIC STRUCTURE PARAMETERS ON DYNAMIC IMPACT ENERGY ABSORPTION

Adeline Petit, Aravind Rajan Ayagara, André Langlet, Rémi Delille, Yves  
Parmantier

► **To cite this version:**

Adeline Petit, Aravind Rajan Ayagara, André Langlet, Rémi Delille, Yves Parmantier. INFLUENCE OF AUXETIC STRUCTURE PARAMETERS ON DYNAMIC IMPACT ENERGY ABSORPTION. XVIth Vibration Engineering & Technology of Machinery Conference (VETOMAC 2021), B.M.S.College of Engineering, Dec 2021, Bengaluru, India. hal-03583095

**HAL Id: hal-03583095**

**<https://hal.science/hal-03583095>**

Submitted on 21 Feb 2022

**HAL** is a multi-disciplinary open access archive for the deposit and dissemination of scientific research documents, whether they are published or not. The documents may come from teaching and research institutions in France or abroad, or from public or private research centers.

L'archive ouverte pluridisciplinaire **HAL**, est destinée au dépôt et à la diffusion de documents scientifiques de niveau recherche, publiés ou non, émanant des établissements d'enseignement et de recherche français ou étrangers, des laboratoires publics ou privés.

## VETOMAC2021-XXX

### INFLUENCE OF AUXETIC STRUCTURE PARAMATERS ON DYNAMIC IMPACT ENERGY ABSORPTION

**Adeline PETIT**

PhD student

Univ. Orléans, Univ. Tours, INSA CVL, LaMé  
63 av de Lattre de Tassigny, 18020 Bourges-France  
Email: adeline.petit@etu.univ-orleans.fr

**Aravind Rajan AYAGARA\***

Associate professor

Dept. of Aeronautical Engineering  
Institute of Aeronautical Engineering  
Dundigal-Hyderabad 500043, Telangana State, India  
Email: a.rajan@iare.ac.in

**André LANGLET**

Associate professor HDR

Univ. Orléans, Univ. Tours, INSA CVL, LaMé  
63 av de Lattre de Tassigny, 18020 Bourges-France  
Email: andre.langlet@univ-orleans.fr

**Rémi DELILLE**

PhD, Research engineer

Univ. Polytechnique Hauts-de-France, LAMIH  
UPHF - 59313 Valenciennes Cedex 9, France  
Email: remi.delille@uphf.fr

**Yves PARMANTIER**

Financial expert

Univ. Orléans, Pôle Capteurs  
63 av de Lattre de Tassigny, 18020 Bourges-France  
Email: yves.parmantier@univ-orleans.fr

#### ABSTRACT

*The present work focuses on the dynamic crushing response of 2D re-entrant auxetic honeycomb by extending previous published models in order to include more design parameters (specific geometrical ratios and/or material properties). If the crushing velocity is constant, the energy absorption occurs at a constant plateau stress up to densification of the structure. An analytical equation based on shock waves propagation analogy in a rigid, perfectly plastic, locking material model is deduced from the study of periodic collapse of the structure. Our analysis enables to theoretically predict the dynamic crushing strength . The formulation depends on the geometric and the material characteristics of the auxetic but also on the impact velocity. Two series of Finite Element simulations of quasi-static and dynamic compressive test of an auxetic structure were carried out using the RADIOSS<sup>TM</sup> explicit solver. The first simulation series consist of a crushing plate loading the structure at a constant imposed velocity (0.5 m/s up to 100 m/s). Results show good accordance between analytical and Finite Element results. The time history of the cell-strain (ratio of deformed cell height to initial cell height) in the crushing direction shows that the peaks observed in the stress-strain curve of the entire structure are linked to complete crushing of each unit cell within a row. The second simulation series replicates the impact of the plate on the structure (initial plate velocities 50 m/s up to 100 m/s). The numerical simulations presented in this study, make it possible to relate the cell-strain, energy absorption and geometrical/material parameters of the auxetic structure.*

**Keywords:** Auxetic structure, impact, Finite Element Model, explicit simulation

\*Address all correspondence to this author.

This is a preprint of the following chapter: PETIT A., AYAGARA A. R., LANGLET A., DELILLE D., PARMANTIER Y., *Influence of auxetic structure paramaters on dynamic impact energy absorption*, published in Vibration Engineering and Technology of Machinery, edited by Rajiv Tiwari, Y. S. Ram Mohan, Ashish K. Darpe, V. Arun Kumar, Mayank Tiwari, 2023, Springer Singapore reproduced with permission of The Editor(s) (if applicable) and The Author(s), under exclusive license to Springer Nature Singapore Pte Ltd. 2024. The final authenticated version will be available online at (due : 07 December 2023) : <https://link.springer.com/book/9789819947201>

## NOMENCLATURE

- AS Auxetic Structure.  
EV Elementary Volume.  
FE Finite Element.  
HS Honeycomb Structure.  
KE Kinetic Energy.  
 $b$  Out-of-plane length ( $Z$ -direction) of the AS [m]  
 $D_0$  Total height ( $Y$ -direction) of the AS [m].  
 $d_{0cell}$  Initial cell height ( $Y$ -direction) [m].  
 $d_{cell}$  Instantaneous cell height ( $Y$ -direction) [m].  
 $D$  Instantaneous total height ( $Y$ -direction) of the AS after time 0 [m].  
 $E$  Young's modulus [Pa].  
 $F$  Force load [N].  
 $h$  Length of the horizontal ( $X$ -direction) cell edge (external face) [m].  
 $H$  Length of the horizontal ( $X$ -direction) cell edge (middle line) [m].  
 $\ell$  Length of the oblique cell edge (external face) [m].  
 $L$  Length of the oblique cell edge (middle line) [m].  
 $M_{max}$  Maximum bending moment [Nm].  
 $M_p$  Fully plastic moment [Nm].  
 $p_{ij}^y$  Momentum of the wall  $ij$  (subscript) in  $Y$ -direction (superscript) [Ns].  
 $S_0$  Auxetic initial transverse ( $X$ - $Z$  plane) area [m<sup>2</sup>].  
 $t$  Cell wall thickness [m].  
 $t_1 - t_0$  Time period for collapse of a row (if no ambiguity is possible,  $t$  will denotes the time) [s].  
 $V$  Volume [m<sup>3</sup>].  
 $v$  Velocity [m s<sup>-1</sup>].  
 $W$  Plastic work [J].  
 $\epsilon_{ds}$  Strain at densification [m m<sup>-1</sup>].  
 $\eta$  Ratio  $H/L$  [m m<sup>-1</sup>].  
 $\theta$  angle between cell edges [rad].  
 $\nu$  Poisson's ratio.  
 $\rho$  Mass density [kg m<sup>-3</sup>].  
 $\sigma$  Stress [Pa].  
 $\sigma_{dyn}$  Dynamic plateau stress [Pa].  
 $\sigma_{stat}$  Static plateau stress [Pa].  
 $\tau$  Ratio  $t/L$  [m m<sup>-1</sup>].

## 1 INTRODUCTION

Cellular materials are known to have multifunctional applications (thermal and noise insulator, lightness, stiffness, high specific strength and so on) and particularly for the energy absorption capacity during an impact [1]. Qualitatively [2], a typical stress-strain curve of cellular materials can be divided in three parts : (i) the elastic part where the curve is quasi-linear, (ii) a plateau interval where the curve is almost "horizontal" (iii) a densification interval where the curve is rising abruptly.

A cellular structure having a long flat stress-strain curve is a good energy absorber according to Ashby *et al.* [2]. This structure deforms plastically at a constant plateau stress until reaching the onset of structure densification. Cellular materials have been widely investigated by Gibson *et al.* [3] who developed an analytical formulation to determine the honeycomb plateau stress under quasi-static compression.

In 1987, Lakes [4] was the first to present a polyurethane foam with a negative Poisson's ratio of  $-0.7$  which was then named "auxetic" by Evans *et al.* [5] in 1991. This specific kind of cellular solid with negative Poisson's ratio raised concern of many researchers. Due to their negative Poisson's ratio, auxetics exhibit horizontal expansion when subjected to vertical traction and shrink horizontally under vertical compression. Compared to conventional cellular structure, auxetic structures have higher shear modulus, better indentation resistance and fracture toughness and, last but not least, a better energy absorption capacity [6]. A great variety of auxetic shapes exists : cellular solid (re-entrant model, chiral model, foams,...), microporous polymers, composites, ceramics, etc.. The re-entrant honeycomb model is one of the most studied. Dong *et al.* [7] examine the influence of cell wall aspect ratio (thickness to a characteristic length ratio) on deformation behavior and on crushing strength during quasi-static compression. Because of their improved mechanical properties compared to classical honeycomb, auxetics are interesting for energy absorption in automotive crashes [8], [9]. Fila *et al.* [10] use Split Hopkinson Pressure Bar to compare specific energy absorption of different auxetic geometry.

In-plane auxetic crushing test is the benchmark analysis to determine quasi-static and dynamic crushing strength of auxetic structures. This strategy is adopted by Ruan *et al.* [11], Hu *et al.* [12, 13], and Hou *et al.* [14] to develop their models.

By considering periodic cells collapse mechanism, Hu *et al.* [12, 13] derived analytical formulation of honeycombs strength during low and high-velocity crushing. Inspired by the results of [12, 13], Hou *et al.* [14] proposed analytical equations for re-entrant auxetic structures under dynamic compression.

In 1993, Reid *et al.* [15], on the basis that wood behave like cellular structure, proposed a shock model for wood using the rigid, perfectly-plastic, locking (r-p-p-l) simplification. This model of the dynamic crushing of cellular structure is validated in 2003 by Ruan *et al.* [11] thanks to numerical in-plane dynamic crushing of honeycombs.

Results of the Finite Elements (FE) simulations at different velocities and for different cell-wall aspect ratio attest the good accordance between theory and simulation. It ensues that with the increase of cell-wall aspect ratio, the crushing strength increases. The same observation can be made with the increase of crushing velocity.

The aim of this study is to extend existing analytical formulations [12, 13], [14] by including more geometrical parameters. Cell-wall angle and cell lengths will be taken into consideration. FE simulations of constant crushing test and impact test have been performed to confirm the analytical formulation and the capability of auxetic structures to absorb kinetic energy (KE). The auxetic responses have been compared with classical honeycomb structures.

## 2 PREDICTION OF AUXETIC STRESS

The auxetic cells configuration called “re-entrant honeycomb” which will be investigated is shown in Fig. 1 including all characteristic data. The neutral axis length (black dotted line in Fig. 1) of the horizontal edge and the bevel of the unit cell are respectively denoted  $H$  and  $L$ . The angle between bevel and horizontal edge is  $\theta$ . The cell-wall thickness is denoted  $t$  and  $b$  is the out-of-plane thickness. The edges  $h$  and  $\ell$  are defined as follow :

$$\ell = L - \frac{t}{2 \sin \theta} \quad (1)$$

$$h = H - \frac{(1 + \cos \theta)t}{\sin \theta} \quad (2)$$

The initial cell height is defined by :

$$d_{0cell} = 2L \sin \theta \quad (3)$$

The total height in the  $Y$ -direction for  $n$  cell rows (layer) is:

$$D_0 = n d_{0cell} + t \quad (4)$$

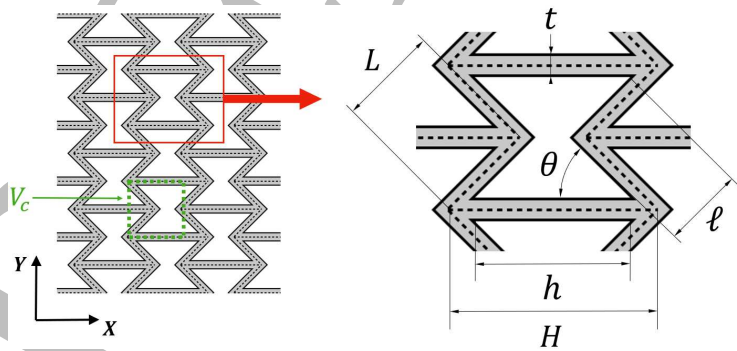


Fig. 1: Re-entrant auxetic cell configuration.

This auxetic structure (abbreviated as “AS”) will be investigated in compression along  $Y$ -axis.

### 2.1 Relative Density And Densification Strain

The relative density of a cellular structure is defined as the ratio of the cellular structure mass density  $\rho_c$  to the mass density  $\rho_s$  of the material of which it is constituted. For the re-entrant honeycomb, it is defined as follow :

$$\frac{\rho_c}{\rho_s} = \frac{V_s}{V_c} \quad (5)$$

where  $V_c$  and  $V_s$  are the cellular structure and material volumes, respectively.

$$V_c = 2bL \sin \theta (H - L \cos \theta) \quad (6)$$

Noting that  $V_s = V_c - V_{void}$  ( $V_{void}$  being the empty volume), we have:

$$V_s = V_c - 2b\ell \sin \theta (h - \ell \cos \theta) \quad (7)$$

From which:

$$\frac{\rho_c}{\rho_s} = 1 - \frac{L \sin \theta - \frac{t}{2}}{L \sin \theta (H - L \cos \theta)} \left[ H - L \cos \theta - \frac{t}{\sin \theta} \left( 1 + \frac{\cos \theta}{2} \right) \right] \quad (8)$$

The relative density can be written in terms of non-dimensional ratio  $\tau$  and  $\eta$ :

$$\tau = t/L \quad (9)$$

$$\eta = H/L \quad (10)$$

$$\frac{\rho_c}{\rho_s} = 1 - \frac{\sin \theta - \frac{\tau}{2}}{\sin \theta (\eta - \cos \theta)} \left[ \eta - \cos \theta - \frac{\tau}{\sin \theta} \left( \frac{1 + \cos \theta}{2} \right) \right] \quad (11)$$

According to the Metal foam Guide [2], a good energy absorber have a high long flat plateau stress. It means that the deformation at which the cellular solid starts the densification must be as high as possible. Densification occurs when stress increases steeply because every cells are crushed. Gibson *et al.* [3] states that the cellular solid is totally densified when the strain is equal to porosity  $1 - \rho_c/\rho_s$ . Therefore the strain at densification is :

$$\epsilon_d^{totally} = 1 - \frac{\rho_c}{\rho_s} \quad (12)$$

Note that if the strain is equal to  $\epsilon_d^{totally}$ , the structure is completely crushed, so that there is no more pore spaces. The densification starts when all cell-walls are in contact. At this stage, there is still some pore spaces, and the strain reaches the value  $\epsilon_{ds}$ . Therefore  $\epsilon_{ds} \leq \epsilon_d^{totally}$ .

The densification starts exactly when  $d_{cell} = 4nt$ . The densification strain  $\epsilon_{ds}$  is therefore expressed as :

$$\epsilon_{ds} = 1 - \frac{(4n+1)t}{D_0} \quad (13)$$

## 2.2 Prediction of Quasi-Static Plateau Stress

The static plateau stress is denoted  $\sigma_{stat}$ . It occurs when cells collapse plastically during compression. This plateau is reached if the made-up materials has a yield strength  $\sigma_y$  and if the bending moment of cell wall reach the fully plastic moment. The plateau stress  $\sigma_{stat}$  of re-entrant honeycomb can be determined using lower-upper bound theorem, as per Gibson *et al.* [1].

Consider a  $Y$ -axis compression. The force causing the plastic collapse stress of the auxetic unit-cell is :

$$F = \sigma_{stat} S_0 = \sigma_{stat} (H - L \cos \theta) b \quad (14)$$

The work done by the load  $F$  during the rotation  $\phi$  of the four plastic hinges of the unit-cell is equal to :

$$W = \sigma_{stat} (H - L \cos \theta) b 2L \phi \cos \theta \quad (15)$$

An upper bound of this work  $W$  is given by equating it to the plastic work of the bending cell wall at the hinges :

$$4M_p \phi \geq \sigma_{stat} (H - L \cos \theta) b 2L \phi \cos \theta \quad (16)$$

where:  $M_p$  is the fully plastic moment ( $M_p = \frac{1}{4} \sigma_y b t^2$ ). It follows that:

$$\sigma_{stat} \leq \sigma_y \frac{\tau^2}{2(\eta - \cos \theta) \cos \theta} \quad (17)$$

A lower bound is given by equating the fully plastic moment to the maximum bending moment in the beam :

$$M_{max} \geq M_p \quad (18)$$

where

$$M_{max} = \frac{1}{2} \sigma_{stat} (H - L \cos \theta) b L \cos \theta \quad (19)$$

It follows that:

$$\sigma_{stat} \geq \sigma_y \frac{\tau^2}{2(\eta - \cos \theta) \cos \theta} \quad (20)$$

Both bounds are equal. That means the exact solution is :

$$\sigma_{stat} = \sigma_y \frac{\tau^2}{2(\eta - \cos \theta) \cos \theta} \quad (21)$$

### 2.3 Prediction of Dynamic Plateau Stress For A Constant Crushing Velocity

Under high-velocity compression, auxetic structures exhibit stress-strain curves and deformation modes significantly different from those at low velocity. It means that the velocity at which the auxetic is crushed have a significant influence on the energy absorption. Many researchers state that under high impact velocity, the deformation mechanism is similar to a crushing wave front propagating through the whole structure. The mechanism could be compared to a shock wave if the auxetic is reduced to a rigid, perfectly plastic, locking material model (r-p-p-l model, [15]). What is now calling dynamic plateau stress  $\sigma_{dyn}$  is theoretically expressed as :

$$\sigma_{dyn} = \sigma_{stat} + C v^2 \quad (22)$$

where  $\sigma_{dyn}$  is the plateau stress at high-velocity compression,  $C$  is a constant that depends of auxetic geometric parameters and  $v$  is the velocity at which the auxetic is crushed.

By following Hou *et al.* [14] research, a theoretical expression of dynamic plateau stress can be derived. Consider an auxetic structure supported by a *rigid* plate at the distal end and crushed at a *constant* high-velocity  $v$  by another *rigid* plate along  $Y$ -axis at proximal end.

As the plates are assumed to be rigid, they do not absorb any strain energy. Thus, this theoretical load case enables to evaluate the maximum capability of energy absorbance up to densification.

As the deformation occurs layer by layer, an elementary volume (EV) representative of a cell's collapse is considered, Fig. 2(a), to develop the equations. The initial EV sizes are :

$$X_0 = 2H - L \cos \theta \quad (23)$$

$$Y_0 = 3L \sin \theta \quad (24)$$

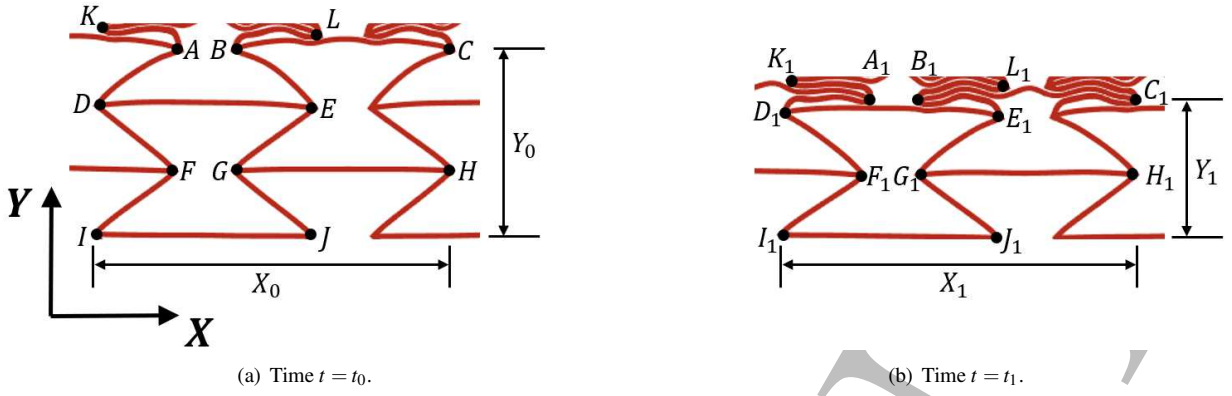


Fig. 2: Collapse of a row.

The collapse period (Fig. 2(a), 2(b)) starts at time  $t = t_0$  and finishes at time  $t = t_1$ . The stresses  $\sigma_1$  and  $\sigma_2$  are the stress applied to the auxetic at proximal end (crushing stress) and at distal end (supporting stress), respectively. Here, the crushing plate moves at constant velocity during the whole collapse period. So,  $\sigma_1$  is considered as a contact stress between the plate and the auxetic, and is also the dynamic plateau stress. During this collapse, cells between EV and the distal end remain unchanged. It could be concluded that the stress at the distal end is equal to the quasi-static plateau stress  $\sigma_{stat}$ . The contraction along  $X$ -axis will be ignored as mentioned by Hou *et al.* [14]. Thus the EV dimensions at time  $t_1$  are:

$$X_1 = X_0 \quad (25)$$

$$Y_1 = 2L \sin \theta + 2t \quad (26)$$

The force applied to the EV by both plates is:

$$F = bX_0(\sigma_1 - \sigma_2) \quad (27)$$

The theorem of linear momentum is applied to the EV during the time period for collapse  $\Delta t = t_1 - t_0$ :

$$F \Delta t = \Delta p = p^1 - p^0 \quad (28)$$

where the momentum of the EV at initial and final state are denoted  $p^0$  and  $p^1$ , respectively. These could be decomposed as a sum of momentum  $p$  along  $Y$ -axis of each wall that compose the EV:

$$p^0 = p_{AD}^y + p_{DE}^y + p_{BE}^y + p_{BC}^y + p_{DF}^y + p_{EG}^y + p_{GH}^y + p_{FI}^y + p_{GJ}^y \quad (29)$$

and

$$p^1 = p_{A_1D_1}^y + p_{D_1E_1}^y + p_{B_1E_1}^y + p_{B_1C_1}^y + p_{D_1F_1}^y + p_{E_1G_1}^y + p_{G_1H_1}^y + p_{F_1I_1}^y + p_{G_1J_1}^y \quad (30)$$

where the  $y$  superscript denotes the momentum direction; the capital subscripts denotes the wall junctions.

Walls  $KA$ ,  $LB$  and  $BC$  are a part of the densified structure. It means that these walls and associated nodes move at velocity  $v$  for the whole period. While nodes  $F$ ,  $G$ ,  $H$ ,  $I$  and  $J$  stay at rest ( $p_{FI} = p_{GJ} = p_{GH} = 0$ ). Walls  $AD$ ,  $BE$  and  $DE$  have joined the densified region at  $t = t_1$ , so  $v_{A_1D_1} = v_{B_1E_1} = v_{D_1E_1} = v$ . As the deformation mode is the same layer by layer, some simplifications could be made between one layer at initial time and the next layer at final time. It leads to:

$$p_{D'F'} = p_{BE}; p_{B'C'} = p_{BC}; p_{E'G'} = p_{AD}; p_{F'I'} = p_{EG}; p_{G'J'} = p_{DF}; p_{G'H'} = p_{DE} \quad (31)$$

The theorem of linear momentum gives:

$$bL_0(\sigma_1 - \sigma_2)\Delta t = \left( p_{A_1D_1}^y + p_{D_1E_1}^y + p_{B_1E_1}^y + p_{B_1C_1}^y + p_{D_1F_1}^y + p_{E_1G_1}^y + p_{G_1H_1}^y + p_{F_1I_1}^y + p_{G_1J_1}^y \right) - \left( p_{AD}^y + p_{DE}^y + p_{BE}^y + p_{BC}^y + p_{DF}^y + p_{EG}^y + p_{GH}^y + p_{FI}^y + p_{GJ}^y \right) \quad (32)$$

$$bL_0(\sigma_1 - \sigma_2)\Delta t = p_{A_1D_1}^y + p_{D_1E_1}^y + p_{B_1E_1}^y \quad (33)$$

As walls  $A_1D_1$ ,  $B_1E_1$  and  $D_1E_1$  have the same velocity that the crushing plate, it results :

$$p_{A_1D_1}^y = p_{B_1E_1}^y = \rho_s b t L v \quad (34)$$

$$p_{D_1E_1}^y = \rho_s b t H v \quad (35)$$

So,

$$\sigma_1 \Delta t = \frac{1}{b(2H - L \cos \theta)} [(p_{A_1D_1}^y + p_{D_1E_1}^y + p_{B_1E_1}^y) + b(2H - L \cos \theta) \sigma_2 \Delta t] \quad (36)$$

$$= \frac{(2\rho_s t L v + \rho_s t H v)}{(2H - L \cos \theta)} + \sigma_2 \Delta t \quad (37)$$

But:

$$\sigma_2 = \sigma_{stat} = \frac{\sigma_y t^2}{2L(H - L \cos \theta) \cos \theta} \quad (38)$$

And:

$$t_1 - t_0 = \frac{|X_1 - X_0|}{v} = \frac{|2L \sin \theta + 2t - 3L \sin \theta|}{v} = \frac{L \sin \theta - 2t}{v} \quad (39)$$

It results:

$$\sigma_{dyn} = \frac{1}{t_1 - t_0} \sigma_1 \Delta t \quad (40)$$

Finally:

$$\sigma_{dyn} = \sigma_{stat} + \frac{\rho_s \tau (2 + \eta)}{(\sin \theta - 2\tau)(2\eta - \cos \theta)} v^2 \quad (41)$$

Stress  $\sigma_{stat}$  will be used to predict the plateau stress under static and quasi-static compression with Eq. (21).

Stress  $\sigma_{dyn}$ , Eq. (41) is for high-velocity compression.

In Eq. (21) and Eq. (41), the depth  $b$  of the AS has no influence. This is because the loading force applied by the moving plate is uniformly distributed over the contact surface.

Some clarifications must be made concerning auxetic design guidelines. First, because of the geometric configuration and the way it deforms, it is easy to understand that the ratio  $h/\ell$  must be greater than 2. It means :

$$\eta \geq 2 + \frac{\tau}{\tan \theta} \quad (42)$$

Then, Eq. (41) for  $\sigma_{dyn}$  is not defined for all values of geometric parameters. Indeed if the ratio  $\tau = t/L$  tends towards  $\frac{1}{2} \sin \theta$  it implies that  $\sigma_{dyn}$  tends towards infinity. This limitation is inherent to the model formulation. It does not mean that the experimental value of  $\sigma_{dyn}$  tends towards infinity.

### 3 FE MODEL OF THE AUXETIC STRUCTURE

A numerical FE model has been developed for evaluating the limits of validity of the analytical formulation when 3D structure are considered. The re-entrant honeycomb model, Fig. 3(a), 3(b), is implemented using the commercial explicit non-linear FE software Radioss<sup>TM</sup> (Altair HyperWorks). The structure is composed of six cells in height  $Y$ -direction and five

cells in horizontal  $X$ -direction. The out-of-plane width  $b$  is  $2.25 \times 10^{-3}$  m ( $Z$ -direction). Cell's sizes are the following :  $H = 12 \times 10^{-3}$  m,  $L = 5.66 \times 10^{-3}$  m,  $t = 0.3 \times 10^{-3}$  m and  $\theta = 45^\circ$ .

The auxetic structure is supported by a fixed steel plate at  $y = 0$ . The auxetic is made of elastic-perfectly plastic aluminium with mass density  $\rho_s = 2700 \text{ kg.m}^{-3}$ , Young's modulus  $E = 6.8 \times 10^{10}$  Pa, yield stress  $\sigma_y = 2,55 \times 10^8$  Pa and Poisson's ratio  $\nu = 0.33$ . The steel plate is assumed to be elastic with mass density  $\rho_s = 7800 \text{ kg.m}^{-3}$ , Young's modulus  $E = 2.10 \times 10^{11}$  Pa, and Poisson's ratio  $\nu = 0.33$ . To mesh the different parts, Under-integrated 8-node hexaedral solid elements with physical hourglass stabilization are chosen. Plates with dimensions of  $2 \times 10^{-3} \times 2.25 \times 10^{-3} \times 80.34 \times 10^{-3}$  m are meshed with  $10^{-3}$  m element length. In the  $X$ - $Y$  plane, the auxetic structure is meshed with  $0.15 \times 10^{-3}$  m elements. In the  $Z$ -direction, the structure is extruded with three elements. The total number of elements is 57378.

The supporting plate is constraint in all directions. The crushing plate is free only in  $Y$ -translation direction.

The auxetic nodes are constraint in  $Z$ -translation direction to avoid out-of-plane displacement. A penalty method general contact is applied to model all interactions (plate/auxetic, auxetic/auxetic). The contact friction is not taken into account.

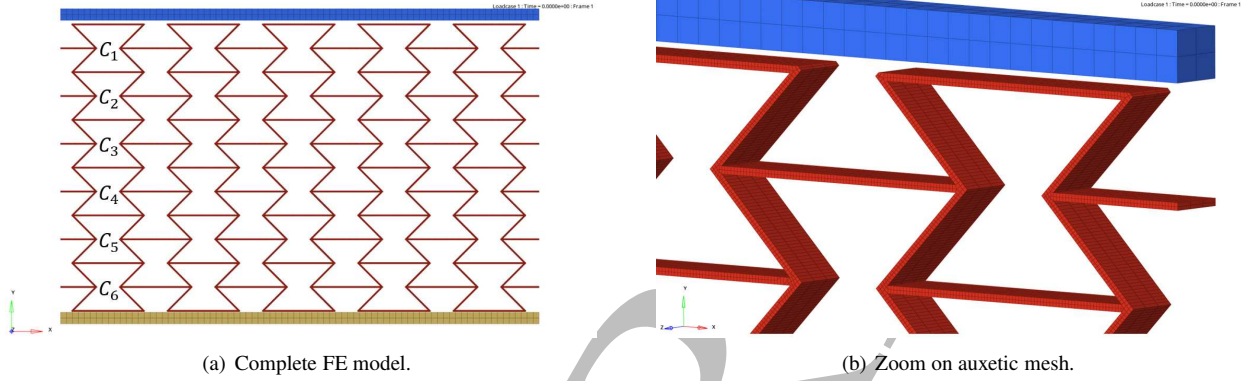


Fig. 3: FE model for crushing simulation.

## 4 RESULTS AND DICUSSION

### 4.1 Auxetic Plateau Stress

First, we consider the crushing of the AS by a plate moving at a constant imposed velocity. The plate is supposed always in contact with the AS. The plateau stress  $\sigma_{dyn}$  is evaluated according to Eq. (41). The dynamic response of the AS obtained trough the FE simulation is expressed in terms of stress  $\sigma$  and strain  $\epsilon$ . The stress  $\sigma$  is calculated by the ratio of the contact force (AS-crushing plate) to the initial transverse ( $X$ - $Z$  plane) area. The strain  $\epsilon$  is defined as the ratio of the absolute value of height variation  $\Delta D$  to the initial height  $D_0$ . In the  $\sigma$ - $\epsilon$ , the constant plateau stress  $\sigma_{dyn}$  is also plotted. For a low velocity  $v = 0.5 \text{ m/s}$  Fig. 4(b) clearly demonstrates that Eq. (21) can be used as a reliable tools for predicting the plateau stress.

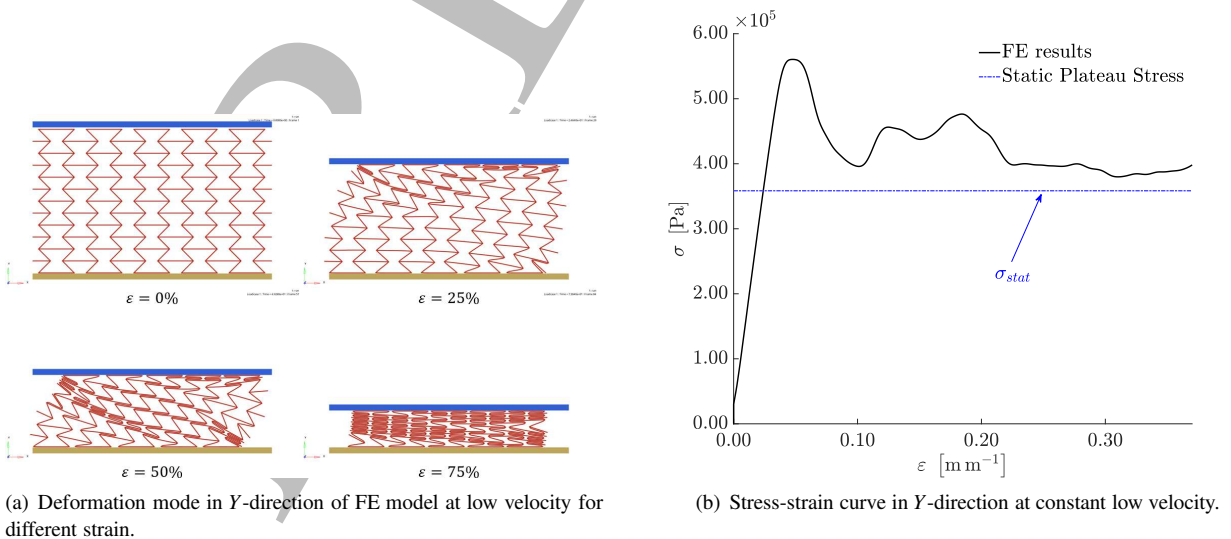


Fig. 4: Results of AS crushing simulation in  $Y$ -direction constant low velocity ( $0.5 \text{ m.s}^{-1}$ ).

For higher velocities, for example  $v = 100$  m/s, oscillation of the stresses and strains due to inertial effects appear in the responses. Fig. 6(b), reveals that the stress  $\sigma$  calculated in the FE simulation oscillates around the plateau stress defined by the analytical formulation. In fact, the oscillations can be explained by analyzing the successive collapse of the layers under the moving plate. Now, let us define the cell-strain as the ratio of the absolute cell height variation  $\Delta d_{cell} = |d_{cell} - d_{0cell}|$  to the initial cell height  $d_{0cell}$ , [13]. Fig. 5 presents the plot of  $\Delta d_{cell}/d_{0cell}$  vs.  $\epsilon$  for each of the 6 rows (horizontal layer) of the structure represented in Fig. 3(a) (model auxetic). When the cell strain of a given row reaches 1, the cell is completely collapsed. If there are  $n$  cell rows the theoretical (analytical) value of densification strain  $\epsilon$  is:

$$\epsilon_{ds} = 1 - \frac{(4n+1)t}{D_0} \quad (43)$$

For  $n = 6$ ,  $t = 0.3$  mm, we expect  $\epsilon_{ds} = 0.85$ , which is exactly what is obtained in the FE results plotted in Fig. 5.

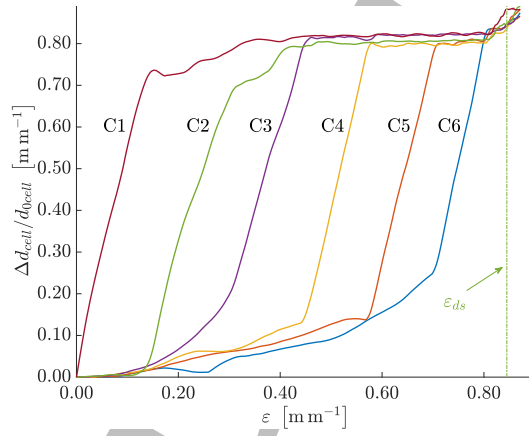


Fig. 5: Cell Strain ( $\Delta d_{cell}/d_{0cell}$ ) vs. strain of AS crushing simulation in  $Y$ -direction constant high velocity ( $100 \text{ ms}^{-1}$ ).

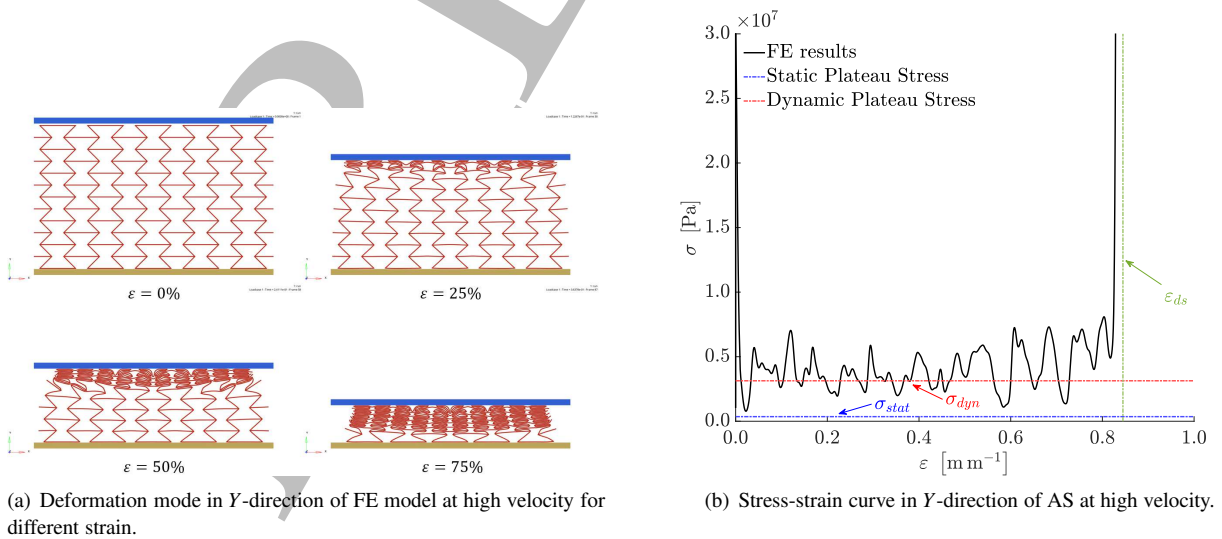
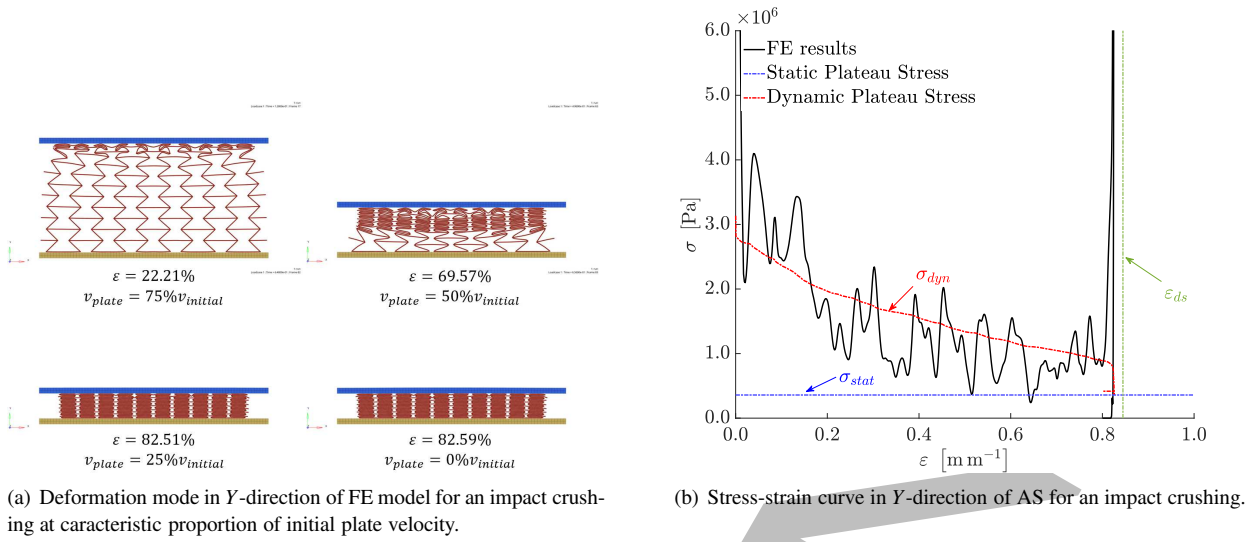


Fig. 6: Results of AS crushing simulation in  $Y$ -direction constant high velocity ( $100 \text{ ms}^{-1}$ ).



**Fig. 7:** Results of AS crushing simulation in Y-direction for an impact crushing ( $100 \text{ m s}^{-1}$ ).

**Secondly**, we consider a steel plate falling on the AS with an initial velocity  $v = 100 \text{ m/s}$ . After impact, the plate dynamic is coupled with the AS response. Fig. 7(a) shows the deformed shape of the AS under the plate. The AS response is also expressed in terms of  $\sigma$ - $\epsilon$ . At various times  $t$  the  $\sigma_{dyn}$  values are calculated with the instantaneous plate velocity  $v(t)$ . It is remarkable that this method leads to accurate prediction of the stress  $\sigma$ . Fig. 7(b) shows the results of the simulation and of the analytical prediction of  $\sigma_{dyn}$  which represent the resistance of the AS to the impacting plate. In this example, the AS is completely collapsed and again, the densification strain reaches the expected value  $\epsilon_{ds} = 0.85$  before the densification interval.

## 4.2 Comparison With Classical Honeycomb Response

According to [12], the static and dynamic plateau stress for honeycombs structure (HS) are respectively:

$$\sigma_{stat} = \frac{2}{3} \sigma_y \tau^2 \quad (44)$$

$$\sigma_{dyn} = \sigma_{stat} + \frac{6\tau\rho_s}{3\sqrt{3}-8\tau} v^2 \quad (45)$$

The procedure applied for the auxetic in the previous sections is also applied for the honeycomb. HS having a total volume equal to that of the AS have been considered. In addition the  $\tau = 53 \times 10^{-3}$  value has been kept equal for the AS and the HS. The mass of the crushing plate is the same for the the AS and the HS.

FE simulations of the HS crushing are presented for a constant velocity in Fig. 8(a), 8(b) and for a falling plate in Fig. 9(a), 9(b). These HS results are to be compared to the AS results presented in Fig. 6(b) ( $100 \text{ m s}^{-1}$ ) and Fig. 7(b) (falling plate).

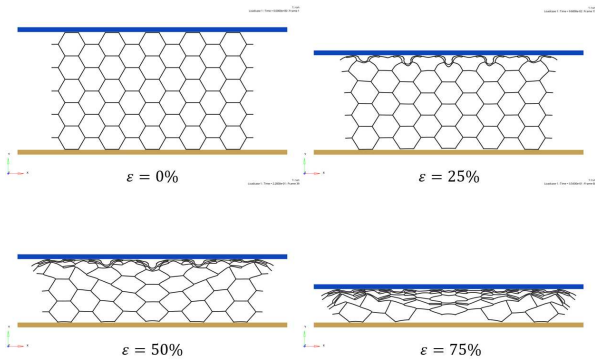
If the plate velocity is constant, the FE results show that during the plateau phase  $\sigma_{dyn}$  is greater for the AS than for the HS. For the AS,  $\sigma_{dyn}$  is calculated according to subsection ???. For the HS, Eq. (45) is used. It is found that for the AS,  $\sigma_{dyn}$  is 38% greater than for the HS.

The strain at densification for HS,  $\epsilon_{ds}$ , is given by:

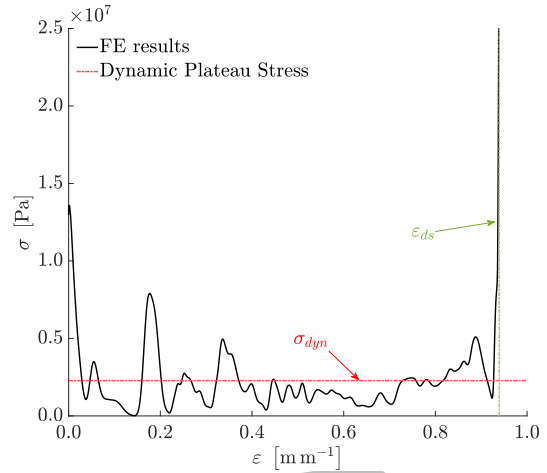
$$\epsilon_{ds} = 1 - \frac{2n}{D_0} t \quad (46)$$

For HS,  $\epsilon_{ds}$  is always greater than for AS, if the number of cells  $n$  in Y-direction is the same (see Eq. (43)).

The energy absorbed in the linear elastic response is small compared to that absorbed in the plastic response. Thus, the maximum energy per unit volume which is absorbed by the AS or the HS can be approximated by the product  $\sigma_{dyn}\epsilon_{ds}$ . Therefore, the design process should provide parameters values (dimensional  $\tau$ ,  $\eta$ ,  $\theta$ , material  $\rho_s$ ,  $\sigma_y$ ) tailored for the specific load cases encountered.

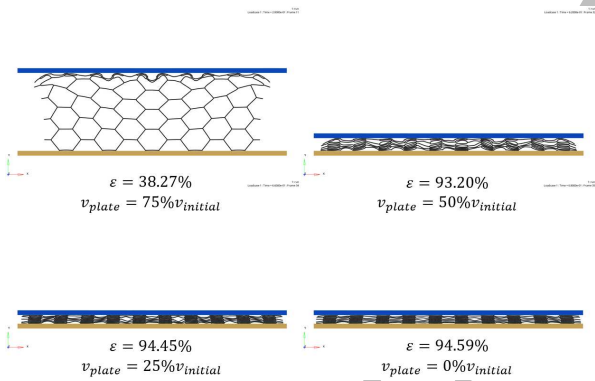


(a) Deformation mode in Y-direction of FE model at high velocity for different strain.

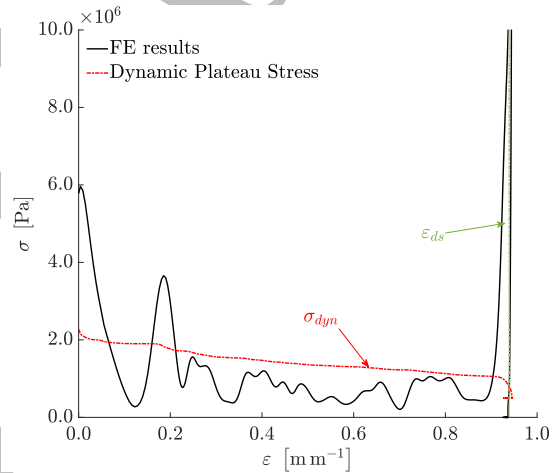


(b) Stress-strain curve in Y-direction of HS at high velocity.

**Fig. 8:** Results of HS crushing simulation in Y-direction constant high velocity ( $100\text{ m s}^{-1}$ ).



(a) Deformation mode in Y-direction of FE model for an impact crushing at characteristic proportion of initial plate velocity.



(b) Stress-strain curve in Y-direction of HS for an impact crushing.

**Fig. 9:** Results of HS crushing simulation in Y-direction for an impact crushing ( $100\text{ m s}^{-1}$ ).

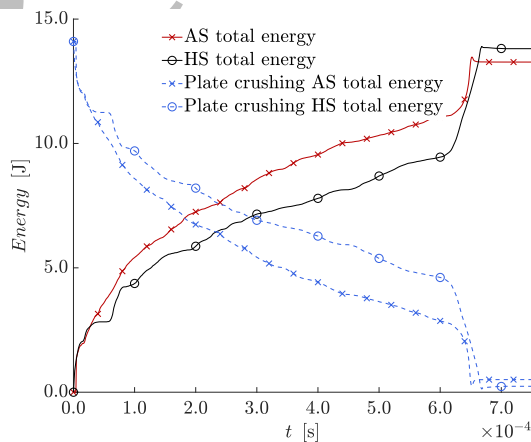


**Fig. 10:** Energy balance of crushing plate and cellular structure for AS and HS simulation.

For the impact load case, the time evolutions of the total energy (internal energy plus kinetic energy) of the AS, the HS, and the plate, are plotted in Fig. 10. Note that as the plate is made of steel, its strain energy is negligible with respect to its KE.

It is found that both the AS and the HS reach densification strain  $\epsilon_{ds}$ . At this strain, the stiffness of the structure increase abruptly, causing the rebound of the plate.

When  $\epsilon_{ds}$  is reached, the energy absorbed by the AS is higher than the energy absorbed by the HS. This is why the KE of the plate impacting the AS is lower than the energy of the plate impacting the HS (Fig. 10).

## 5 CONCLUSION

In this paper, a closed-form formula has been proposed for predicting the plateau stress of architected auxetic lattices during imposed velocity crushing, or impact crushing.

The equations inspired by the articles of Hu *et al.* [12] and Hou *et al.* [14] were adapted in order to explicitly take into account cell geometrical ratios: thickness to oblique length ratio ( $\tau$ ), horizontal to oblique length ratio ( $\eta$ ), wall angle ( $\theta$ ).

The analytical formula were validated thanks to Finite Element simulations.

It is then possible to optimize the geometrical and material parameters in order to tailor the energy absorption ability for facing specific load case.

In-depth studies are in progress to validate the enhanced performance of auxetic lattices relatively to classical architected structures (as honeycombs) in terms of energy absorption.

## ACKNOWLEDGMENT

The authors acknowledge the french Région Centre-Val de Loire for having provided the funds for the study under the project AxSur.

## REFERENCES

- [1] Gibson LJ, Ashby MF, Schajer GS, Robertson CL. The Mechanics of Two-Dimensional Cellular Materials. Proceedings of the Royal Society of London Series A, Mathematical and Physical Sciences. 1982;382(1782):25–42. <https://doi.org/10.1098/rspa.1982.0087>.
- [2] Ashby MF, Evans AG, Fleck NA, Gibson LJ, Hutchinson JW, Wadley HNG. Metal Foams: A Design Guide. Butterworth-Heinemann, Woburn; 2000.
- [3] Gibson LJ, Ashby MF. Cellular Solids: Structure and Properties. 2nd ed. Cambridge Solid State Science Series. Cambridge University Press; 1997. <https://doi.org/10.1017/CBO9781139878326>.
- [4] Lakes R. Foam Structures with a Negative Poisson's Ratio. Science. 1987;235(4792):1038 – 1040. <https://doi.org/10.1126/science.235.4792.1038>.
- [5] Evans KE, Nkansah MA, Hutchinson IJ, Rogers SC. Molecular Network Design. Nature. 1991;353:124. <https://doi.org/10.1038/353124a0>.
- [6] Carneiro V, Meireles J, Puga H. Auxetic materials - A review. Materials Science-Poland. 2013;31:561–571. <https://doi.org/10.2478/s13536-013-0140-6>.
- [7] Dong Z, Li Y, Zhao T, Wu W, Xiao D, Liang J. Experimental and Numerical Studies on the Compressive Mechanical Properties of the Metallic Auxetic Reentrant Honeycomb. Materials & Design. 2019;182:108036. <https://doi.org/10.1016/j.matdes.2019.108036>.
- [8] Simpson J, Kazanci Z. Crushing investigation of crash boxes filled with honeycomb and re-entrant (auxetic) lattices. Thin-Walled Structures. 2020;150:106676. <https://doi.org/10.1016/j.tws.2020.106676>.
- [9] Abdullah NAZ, Sani MSM, Salwani MS, Husain NA. A review on crashworthiness studies of crash box structure. Thin-Walled Structures. 2020;153:106795. <https://doi.org/10.1016/j.tws.2020.106795>.
- [10] Fíla T, Zlámál P, Jiroušek O, Falta J, Koudelka P, Kytýř D, et al. Impact Testing of Polymer-Filled Auxetics Using Split Hopkinson Pressure Bar: Impact Testing of Polymer-Filled Auxetics. Advanced Engineering Materials. 2017;19:1700076. <https://doi.org/10.1002/adem.201700076>.
- [11] Ruan D, Lu G, Wang B, Yu TX. In-Plane Dynamic Crushing of Honeycombs - a Finite Element Study. International Journal of Impact Engineering. 2003;28(2):161 – 182. [https://doi.org/10.1016/S0734-743X\(02\)00056-8](https://doi.org/10.1016/S0734-743X(02)00056-8).
- [12] Hu LL, Yu TX. Dynamic Crushing Strength of Hexagonal Honeycombs. International Journal of Impact Engineering. 2010;37(5):467 – 474. <https://doi.org/10.1016/j.ijimpeng.2009.12.001>.
- [13] Hu LL, Yu TX. Mechanical Behavior of Hexagonal Honeycombs under Low-Velocity Impact - Theory and Simulations. International Journal of Solids and Structures. 2013;50:3152 – 3165. <https://doi.org/10.1016/j.ijsolstr.2013.05.017>.
- [14] Hou X, Deng Z, Zhang K. Dynamic Crushing Strength Analysis of Auxetic Honeycombs. Acta Mechanica Solida Sinica. 2016;29(5):490 – 501. [https://doi.org/10.1016/S0894-9166\(16\)30267-1](https://doi.org/10.1016/S0894-9166(16)30267-1).
- [15] Reid SR, Peng C. Dynamic Uniaxial Crushing of Wood. International Journal of Impact Engineering. 1997;19(5-6):531 – 570. [https://doi.org/10.1016/S0734-743X\(97\)00016-X](https://doi.org/10.1016/S0734-743X(97)00016-X).